SCIENTIFIC REPORTS

OPEN

SUBJECT AREAS:
CALCIUM SIGNALLING
CELLULAR NEUROSCIENCE
MOLECULAR NEUROSCIENCE

Received
30 September 2013

Accepted
16 April 2014

Published
19 June 2014

Correspondence and requests for materials should be addressed to T.S. (ta_sugiyama@ot.olympus.co.jp)

Light-induced rapid Ca^{2+} response and MAPK phosphorylation in the cells heterologously expressing human OPN5

Takashi Sugiyama, Hirobumi Suzuki & Takeo Takahashi

Corporate R&D Center, Olympus Corporation, Tokyo, Japan.

Molecular imaging is a powerful tool for investigating intracellular signalling, but it is difficult to acquire conventional fluorescence imaging from photoreceptive cells. Here we demonstrated that human opsin5 (OPN5) photoreceptor mediates light-induced Ca^{2+} response in human embryonic kidney (HEK293) and mouse neuroblastoma (Neuro2a) cell lines using a luminescence imaging system with a fluorescent indicator and a newly synthesized bioluminescent indicator. Weak light fluorescence and bioluminescence imaging revealed rapid and transient light-stimulated Ca^{2+} release from thapsigargin-sensitive Ca^{2+} stores, whereas long-lasting Ca^{2+} elevation was observed using a conventional fluorescence imaging system. Bioluminescence imaging also demonstrated that OPN5 activation in HEK293 cells induced a decrease in pertussis toxin–sensitive cAMP, confirming previous reports. In addition, ultraviolet radiation induced the phosphorylation of mitogen-activated protein kinases when OPN5 was stimulated in Neuro2a cells. These findings suggest that the combination of these imaging approaches may provide a new means to investigate the physiological characteristics of photoreceptors.

Opsins are photoreceptive proteins that transduce external light signals into intracellular signals in both visual and non-visual photoreception in animals. Among the opsin family members, Opsin5/neuropsin (OPN5) has a unique localization pattern, biophysical characteristics, and function in several animal species and retinal ganglion cell lines (RGC-5)[1–6]. Japanese quail (*Coturnix japonica*) OPN5 acts as a G protein–coupled receptor to induce Ca^{2+} flux and control seasonal reproduction[2]. Chicken (*Gallus gallus domesticus*) OPN5 is a ultraviolet (UV)-sensitive bistable photopigment that couples with G_i-type G proteins[5]. The absorption maxima of quail OPN5 is approximately 420 nm, and the absorption maxima of the chicken OPN5 is estimated to be 360 nm for the non-irradiated protein and 474 nm for the UV-irradiated protein. Although quail OPN5 is associated with Ca^{2+} signalling cascade, suggesting the involvement of G_q-type G proteins[2] and OPN5-expressing rat RGC-5 cells show Ca^{2+} responses to light stimulation[6], this relationship with Ca^{2+} signaling has not been demonstrated in other species. Knockdown of OPN5 via small interfering RNA in mediobasal hypothalamus of border canary (*Serinus canaria*) inhibits photo-induced expression of thyrotropin-stimulating hormone β-subunit, a critical step in the control of reproduction in birds[7]. In mammals, homologs of OPN5 gene have been identified in mouse (*Mus musculus*) and human genomes, and the corresponding proteins are expressed in neural tissue[3]. Both mouse and human OPN5 act as UV-sensitive photoreceptors linked to G_i-type G proteins, with absorption maxima in the UV (380 nm) and visible regions (471 nm), and OPN5 has been detected in retina, brain, and the outer ear in mice[1]. These results suggest that UV light may regulate some G protein–related physiological processes in humans. Hence, we were interested in identifying the signalling molecules downstream of human OPN5 upon photo-activation.

Alterations in signalling molecules involved in light-mediated responses can give rise to changes in gene expression as well as in the activation of transcription factors[8,9]. The highly conserved mitogen-activated protein kinase (MAPK) family of signalling molecules are involved in the response to growth-stimulatory signals as well as to adverse conditions, such as exposure to cytotoxic and genotoxic substances and radiation. Green light-emitting diode light has been shown to activate three types of MAPKs, namely extracellular signal-regulated kinases (ERKs), p38 MAPKs, and Jun amino-terminal kinases (JNK)/stress-activated protein kinases (SAPKs) in orbital fat stem cells[9], and the MEK-specific inhibitor U0126 drastically blocked the expression of light-induced *period2* homolog in a zebrafish (*Danio rerio*) cell line[10], implicating the MAPK pathway in light-induced signalling.

Molecular imaging is a powerful tool for investigating intracellular signal transduction, but it may be difficult to employ fluorescence indicators in photoreceptive or photosensitive cells. Bioluminescence imaging of live cells has been improved to be an alternative to fluorescence imaging in these cases because it does not require exogenous illumination[11]. In this study, we developed luciferase-based bioluminescent indicators for Ca^{2+} and cAMP and visualized light-induced Ca^{2+} and cAMP dynamics in human OPN5-expressing human embryonic kidney (HEK293) and mouse neuroblastoma (Neuro2a) cell lines under constant dark conditions. We also showed that OPN5-mediated transient Ca^{2+} response was confirmed by using weak light fluorescence imaging technique, but not by using a conventional fluorescence imaging system with brighter excitation light. In addition, UV radiation induced the phosphorylation of ERKs, p38, and JNK/SAPKs when OPN5 was reconstituted with 11-*cis*-retinal in the dark. These findings suggest that weak light fluorescence and bioluminescence imaging techniques may provide a new approach to investigate the physiological characteristics of photoreceptors, and OPN5 may influence the gene expression through MAPK signaling cascade.

Results

Conventional fluorescence imaging of light-induced Ca^{2+} response in OPN5-expressing HEK293 cells. To assess the relationship between human OPN5 and intracellular signaling cascades, we established HEK293 and Neuro2a cell lines stably expressing human OPN5 (Fig. 1a). Initially, we performed fluorescence Ca^{2+} imaging assay using the indicators Fluo-4 and Calcium Orange. OPN5-expressing HEK293 cells loaded with Fluo-4 were excited (470–490 nm), and emission was detected at 510 nm. Unexpectedly, excitation of the fluorophore caused a light-induced spike in Fluo-4 fluorescence interpreted as Ca^{2+} flux in OPN5-expressing cells, whereas illumination with UV light (385–400 nm) did not affect the intracellular Ca^{2+} concentrations (Fig. 1b). The excitation wavelength range of Fluo-4 encompasses the blue-light absorption maxima for human OPN5 photoproduct (λ_{max} = 471 nm; see Supplementary Fig. S1 online); however, there are no reports supporting whether activation of the OPN5 photoproduct by blue light activates G proteins. Nevertheless, it is possible that the excitation light was sufficiently bright to activate the UV-absorbing pigment on its long-wavelength flank. To avoid unintentional activation of OPN5, the red-shifted Ca^{2+} indicator, Calcium Orange, was also used for imaging light-induced Ca^{2+} response. The longer wavelength light (520–550 nm) required for the excitation of Calcium Orange dye did not activate any downstream G protein[5]. Calcium Orange fluorescence was stable at the excitation wavelength, and stimulation with bright UV light (>3.2 mW/mm^2) induced a sustained intracellular Ca^{2+} increase (Fig. 1c) for more than 15 min. Although these imaging experiments revealed that human OPN5 photoreceptor is linked to intracellular Ca^{2+} signalling, we found that the brightness of the light required for the activation of OPN5 was much higher than previously reported levels[1].

Luciferase-based indicators for signalling molecules and bioluminescence imaging. To overcome the problem of unintentional activation of cellular processes upon excitation with light in conventional fluorescence imaging, we constructed two bioluminescent indicators modelled after established luciferase-based indicators for Ca^{2+} [12] and cAMP[13–16] (reviewed in [11]; Fig. 2a). These indicators contained a calmodulin-M13 Ca^{2+} sensor domain (cpGL-CaM) or a mouse protein kinase-A regulatory subunit cAMP-binding domain (cpGL-α-CT) fused to firefly luciferase. Characterisation of these indicators was performed using the purified histidine-tagged proteins expressed in bacteria. We monitored the intensity of the bioluminescence of these indicators after addition of varying concentrations of Ca^{2+} or cAMP, and it was revealed that the intensity was altered in a dose-dependent manner. Bioluminescent Ca^{2+} indicator (cpGL-CaM) showed a gradual decrease in the luminescence, reflecting the increasing Ca^{2+} concentration with Kd value = 165 nM (Fig. 2b). The Ca^{2+} affinity of this indicator was slightly higher than that of the fluorescent indicators used (Kd values for Fluo-4 and Calcium Orange are 345 nM and 185 nM, respectively). However, the bioluminescence of cAMP indicator (cpGL-α-CT) increased when cAMP concentration increased (Fig. 2C). The bioluminescence was not altered at submicromolar range of cGMP, indicating the specificity of the change in bioluminescence (EC_{50} of 19.2 nM for cAMP; 3.2 μM for cGMP). A change in the bioluminescence is an indication of the conformational change that occurred in the Ca^{2+}- or cAMP-binding domain. To test the utility for bioluminescence imaging in intact mammalian cells, the mammalian expression vector containing either Ca^{2+} or cAMP indicator were transfected into wild-type HEK293 cells. The cells were maintained in the dark, and their luminescence was visualized after addition of luciferin. Single-cell images taken with 5–10 s exposures indicated that both constructs were localized to the cytoplasm. For temporal analysis of the changes in bioluminescence, images were obtained every 10–15 s. The bioluminescence of cpGL-CaM-expressing cells was observed when Ca^{2+} flux was induced by the activation of P2 purine receptor with ATP. The bioluminescence transiently decreased after the addition of ATP, and some cells showed subsequent oscillatory changes in the luminescence (Fig. 2d). Bioluminescence of the indicator fluctuated before stimulation, but large decreases in the luminescence were observed after stimulation. When the amplitude of the changes in luminescence was 3-times greater than the standard deviation of baseline fluctuation, it was considered as a ligand-induced response (see Supplementary Fig. S2 online). ATP-induced Ca^{2+} response was confirmed by conventional fluorescence imaging with Fluo-4 (Fig. 2e) and Calcium Orange (see Supplementary Fig. S3 online) dyes in HEK293 cells. Next, forskolin, a cAMP-increasing reagent, induced an increase in the intensity of the luminescence of cpGL-α-CT-expressing HEK293 cells (Fig. 2f). These results demonstrate that bioluminescence imaging can indicate the modifications in the intracellular Ca^{2+} and cAMP concentrations in drug-stimulated HEK293 cells, even if the temporal resolution is more than 10 s.

Light-activated OPN5 affects intracellular Ca^{2+} and cAMP signaling in HEK293 cells. Using the luminescent indicator, Ca^{2+} dynamics associated with light-induced OPN5 were measured. OPN5-expressing HEK293 and Neuro2a cells were transfected with cpGL-CaM expression vector, and the luminescence was visualized. Upon 10-s stimulation with UV light through band-pass filter (385–400 nm; 0.2 μW/mm^2), a transient decrease in luminescence was observed in HEK293 (Fig. 3a) and Neuro2a (Fig. 3e) cells containing 11-*cis*-retinal-reconstituted OPN5. Over 90% of OPN5-expressing HEK293 cells (Fig. 3m) and 55% of OPN5-expressing Neuro2a cells (Fig. 3n) showed the light-induced change in bioluminescence. Without retinal reconstitution, however, the number of light-responding cells decreased in both the cell lines (22% of HEK293 cells (Fig. 3m) and 3% of Neuro2a cells (Fig. 3n)), and the amplitude of changes in bioluminescence also decreased in OPN5-expressing HEK293 cells and Neuro2a cells (Fig. 3o and p). Empty-vector-transfected HEK293 and Neuro2a cells have never been observed with light-induced changes in bioluminescence of the indicator (Fig. 3c, d, g, and h). These results suggested that submicro-watt light was adequate to induce Ca^{2+} flux in bioluminescence imaging (constant dark) in OPN5-expressing HEK293 and Neuro2a cells after 11-*cis*-retinal reconstitution. Optical power of excitation light for conventional fluorescence imaging was over 1 mW/mm^2 in this report, and we hypothesized that the bright excitation light for Fluo-4 could affect the OPN5 photoreceptor. To test this hypothesis, we performed a weak light Fluo-4

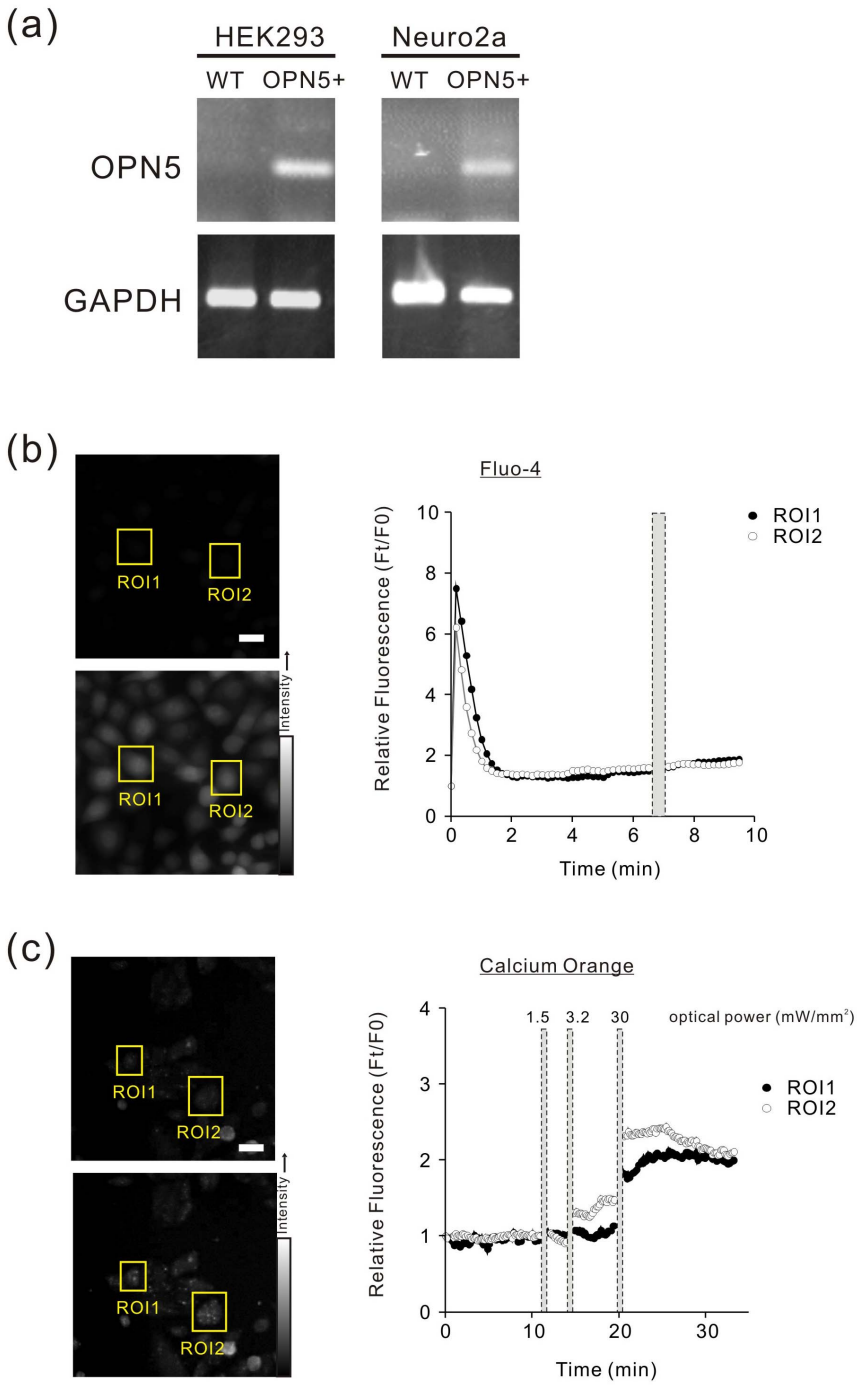

Figure 1 | Intracellular Ca^{2+} imaging using fluorescence indicators in OPN5-expressing HEK293 cells. (a) Total RNA from empty vector–transfected (WT) or the human OPN5-transfected (OPN5+) HEK293 and Neuro2a cells was subjected to RT-PCR, and the products were analysed by performing agarose gel electrophoresis. The control GAPDH gene was equally expressed in both cell types. The full length gels were presented in Supplementary Fig. S5. (b) Fluorescence images of fluo-4-loaded OPN5-expressing HEK293 cells (left, upper image) were acquired every 10 s. The fluorescence intensity of each cell (each region of interest, ROI) was calculated relative to the fluorescence measured at the beginning of imaging (Ft/F0) and was plotted temporally. The cells were illuminated using UV light (350–380 nm; 20 mW/mm^2 optical power) for 30 s at the time indicated in the shaded region. (c) A red-shifted Ca^{2+} indicator, Calcium Orange, was used to track light-induced Ca^{2+} signalling in OPN5-expressing HEK293 cells. Fluorescence images acquired before stimulation (upper image) and after UV light illumination (lower image) are shown. Shaded regions in the trace indicate illumination with UV light for 30 s at weak (1.5 mW/mm^2), moderate (3.2 mW/mm^2), and high (30 mW/mm^2) optical power. Temporal changes in fluorescence intensity are shown in the trace. Representative data from 4 independent experiments for each dye is presented. Bars = 20 μm.

fluorescence imaging using the luminescence imaging system. Fluo-4-loaded cells were excited by weak light from halogen lamp through a band-pass filter (470–490 nm; 0.05 $\mu W/mm^2$) and ATP-induced transient increase in fluorescence was observed in OPN5-expressing cells (see Supplementary Fig. S4 online). These results suggested that the power of the weak light (0.05 $\mu W/mm^2$) was adequate to excite Fluo-4 without activating OPN5 during the imaging. Upon 10-s stimulation with UV light through band-pass filter (385–400 nm; 0.2 $\mu W/mm^2$), a transient increase in fluorescence was observed in HEK293 cells containing 11-*cis*-retinal-reconstituted OPN5 (Fig. 3i),

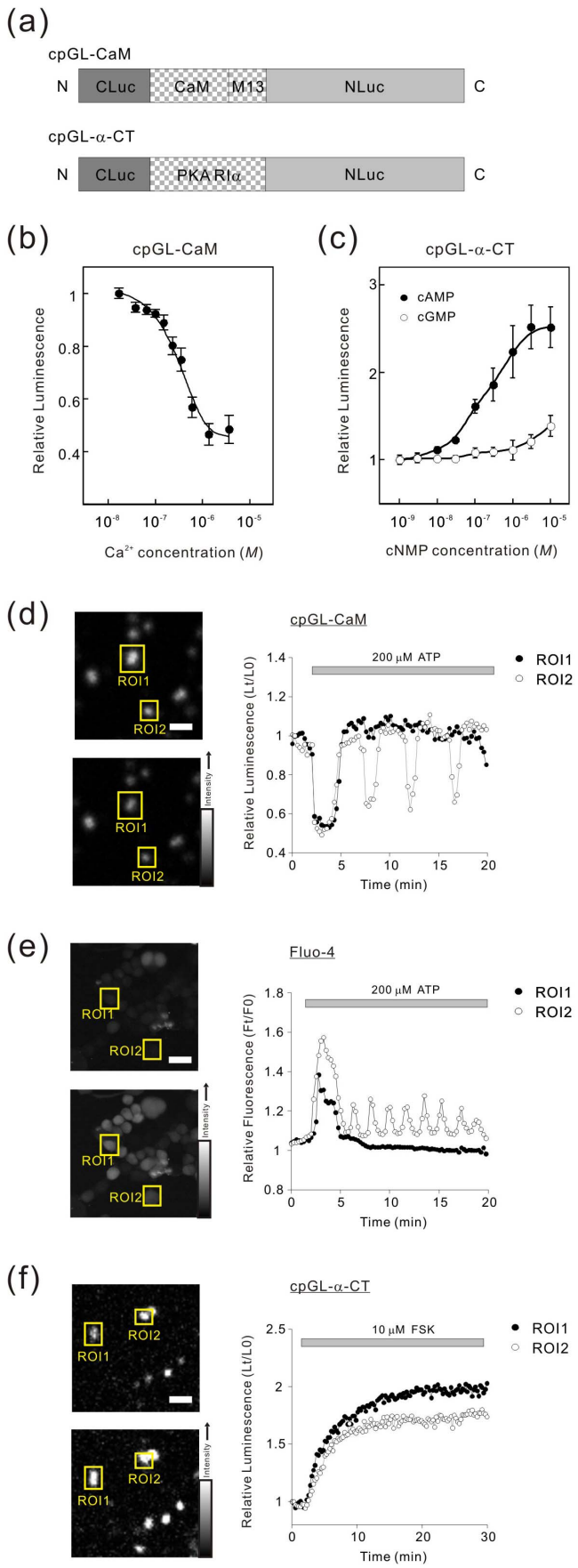

Figure 2 | Bioluminescence indicators for intracellular second messengers. (a) Domain structure of cpGL-CaM and cpGL-α-CT. Purified His-tag proteins (1 μg of each) for cpGL-CaM (b) and cpGL-α-CT (c) were incubated with the indicated concentrations of Ca^{2+} or cNMP (cAMP (filled circle) or cGMP (open circle)) for 15 min at ~24°C, following which the bioluminescence was measured. The data shown is representative of 4 independent experiments, with each determination performed in duplicate, and the values are expressed as mean ± SD. (d) Expression vector for cpGL-CaM was introduced into HEK293 cells, and the cells were supplemented with 2 mM D-luciferin and treated with 200 μM ATP. Single-cell bioluminescence images were obtained every 15 s (5–10 s exposure per image). (e) Typical Ca^{2+} response in ATP-activated HEK293 cells recorded by Fluo-4 fluorescence imaging. (f) Ten μM forskolin (FSK) increased the bioluminescence of cpGL-α-CT-introduced HEK293 cells. The luminescence or fluorescence intensities were calculated relative to the luminescence or fluorescence measured at the beginning of imaging (Lt/L0 or Ft/F0) for the cells in the indicated regions of interest (ROIs) as shown in the trace. Representative images acquired before (upper left) and after (lower left) drug application are shown. Typical temporal responses (right; decreasing luminescence for cpGL-CaM (d), or increasing signal for Fluo-4 (e) and cpGL-α-CT (f)) for cells in the indicated ROIs are plotted. Representative imaging data are from 4 independent experiments for each indicator. Bars = 50 μm.

and a slight increase was observed in cells without 11-*cis*-retinal (Fig. 3j). The Ca^{2+} responses were similar to those observed in bioluminescence imaging (Fig. 3a). Empty-vector-transfected HEK293 cells have never been observed with light-induced changes in fluorescence of the indicator (Fig. 3k and l).

Both bioluminescence imaging and weak light fluorescence imaging revealed that submicro-watt light induced Ca^{2+} signalling through OPN5, whereas brighter light (>3.2 mW/mm^2) was needed for OPN5 activation in the conventional fluorescence imaging using calcium orange, and the light-induced Ca^{2+} increase lasted for over 15 min. To determine the repeatability of light-induced Ca^{2+} signals, the cells were exposed to repetitive light pulses at 1-min intervals. Almost all the light-sensitive cells continued to respond to the repetitive light stimulation (Fig. 4a). To confirm that these bioluminescence changes were dependent on Ca^{2+} flux, cells loaded with 1,2-bis(2-aminophenoxy)ethane-N,N,N′,N′-tetraacetic acid tetrakis (BAPTA), a Ca^{2+} chelator, were illuminated with UV light and the changes in luminescence were monitored. The illumination did not affect the bioluminescence of indicator (Fig. 4b), suggesting that the changes in luminescence indicated the changes in Ca^{2+} dynamics. To clarify the Ca^{2+} source for human OPN5, the effect of depletion of Ca^{2+} stores by thapsigargin was examined. An increase in Ca^{2+} was observed in response to thapsigargin treatment, but subsequent light stimulation no longer affected intracellular Ca^{2+} concentrations after thapsigargin treatment (Fig. 4c). These results suggested that OPN5 influences the signalling mechanisms to release Ca^{2+} from intracellular Ca^{2+} stores.

OPN5 activation decreases intracellular cAMP concentrations[1,5]. To ascertain whether bioluminescence imaging could detect this decrease in cAMP, OPN5-expressing cells were transfected with cpGL-α-CT, and the luminescence was observed after activation with light. Cellular luminescence was increased by forskolin, and subsequent UV illumination induced 5% decrease in the bioluminescence transiently (Fig. 5a). Although the forskolin-induced increase in luminescence was observed after treatment with G_i-type G-protein blocker, pertussis toxin, the light-induced decay of the bioluminescence was inhibited (Fig. 5b and c). These results suggest that bioluminescence imaging was suitable for detecting OPN5-mediated changes in intracellular cAMP concentration.

Activation of OPN5 induces phosphorylation of mitogen-activated protein kinases (MAPKs) in Neuro2a cells. Next, we investigated the link between transcription factor activation and light-activated OPN5 in neuronal Neuro2a cells by western blot analysis. To determine whether MAPK activation occurs in OPN5-

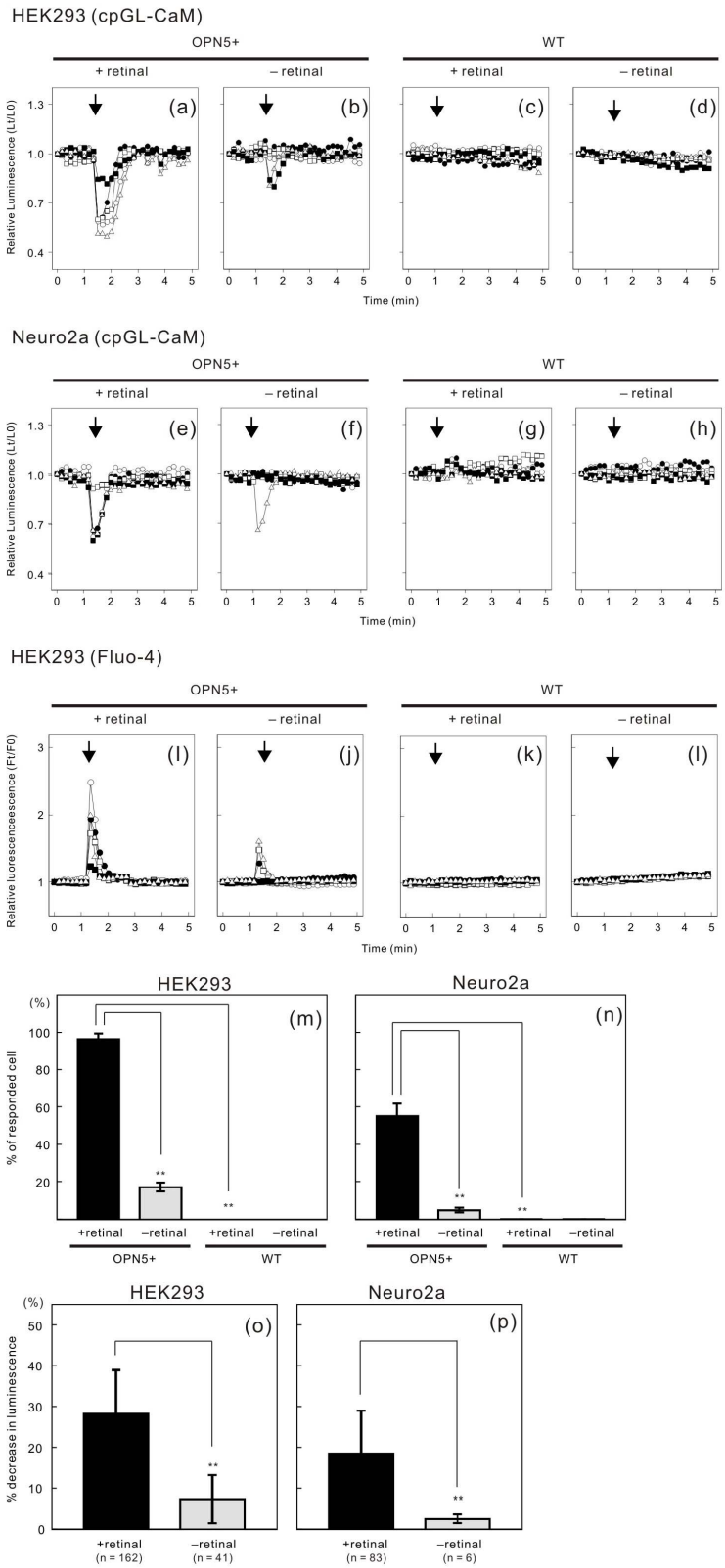

Figure 3 | Ca^{2+} responses after light stimulation of human OPN5-expressing cells. Changes in relative bioluminescence or fluorescence signals (Lt/L0 or Ft/F0) in 5 individual cells in response to UV light pulse (385–400 μm; 10 s at 0.2 μW/mm^2; arrows) are shown. For bioluminescence imaging, OPN5-expressing (OPN5+) or empty-vector-transfected (WT) HEK293 cells (a–d) and Neuro2a cells (e–h) were transfected with cpGL-CaM, and treated with luciferin (2 mM) and with (+retinal) or without (-retinal) 11-*cis*-retinal (5 μM). For fluorescence imaging, OPN5-expressing or empty-vector-transfected (WT) HEK293 cells (i–l) were loaded with Fluo-4 dye (5 μM) and treated with or without 11-cis-retinal (5 μM). Representative traces are from 4 independent imaging experiments. Averaged numbers of UV light-responding cells in OPN5-expressing HEK293 (m) and Neuro2a (n) cells increased after treatment with 11-*cis*-retinal (vs untreated or WT cells; n = 4; $^{**}p < 0.01$). Reduction in luminescence was also increased in retinal-treated OPN5-expressing HEK293 (o) and Neuro2a (p) (retinal-treated vs untreated cells; $^{**}p < 0.01$).

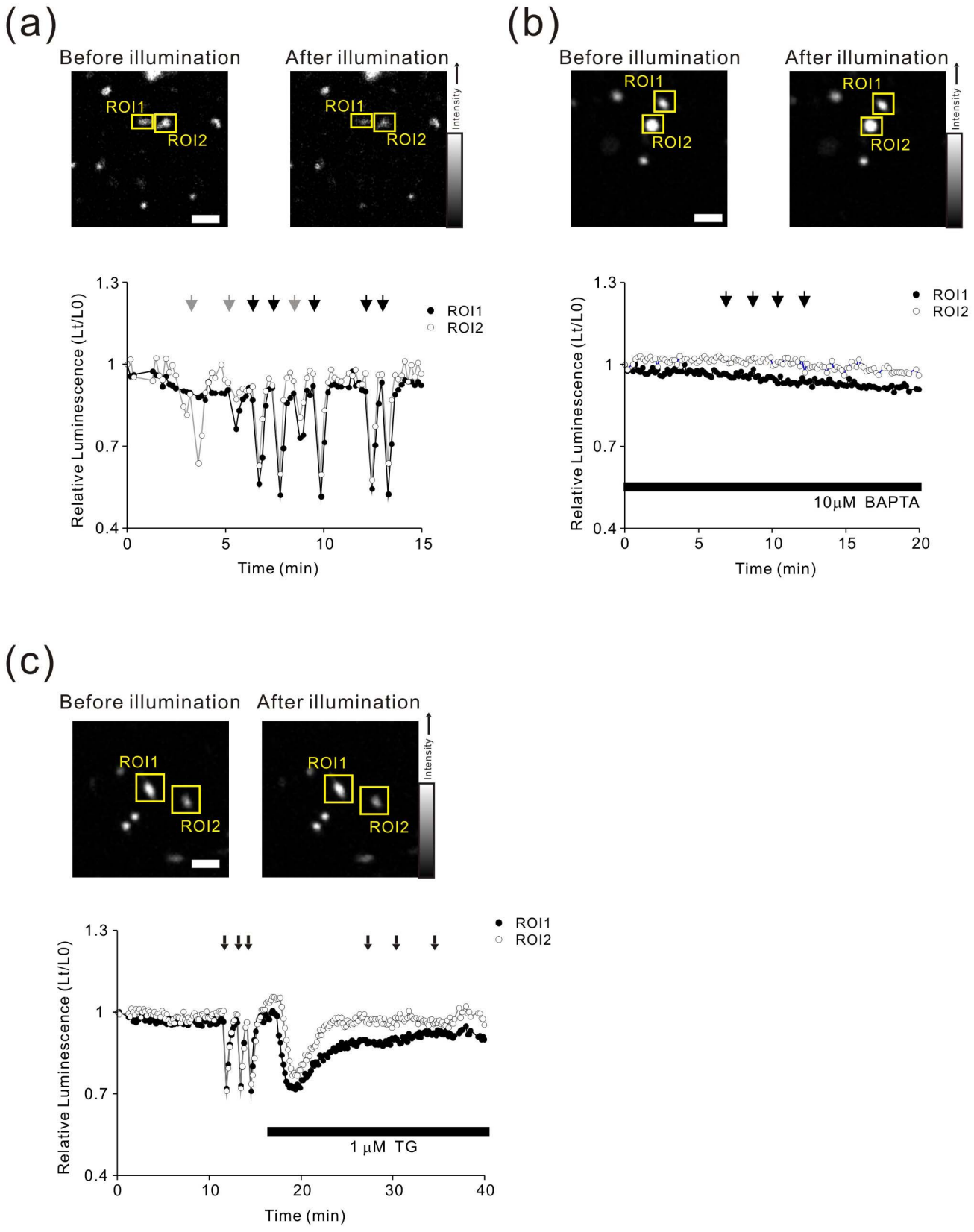

Figure 4 | Ca^{2+} responses after light stimulation of human OPN5-expressing cells. (a) OPN5-expressing cells were transfected with cpGL-CaM and treated with 11-*cis*-retinal (5 μM) and luciferin (2 mM). Luminescence images were acquired every 10 s. Representative bioluminescence images acquired before (left) and after (right) UV light illumination (385–400 nm) are shown. Relative bioluminescence signals (Lt/L0) decreased moderately after weak UV light pulses (10 s at 0.1 μW/mm^2; grey arrows) and decreased more dramatically with higher energy UV light pulses (10 s at 0.2 μW/mm^2; black arrows). (b) As a control, BAPTA AM was applied to the cells 60 min before the imaging and UV light stimulation (10 s at 0.2 μW/mm^2; black arrows). (c) In the presence of thapsigargin (1 μM; TG; black bar), a Ca^{2+} store depletion reagent, UV light (10 s at 0.2 μW/mm^2)-induced decrease in bioluminescence (arrows) was not observed. Representative imaging data are from 4 independent experiments. Bars = 50 μm.

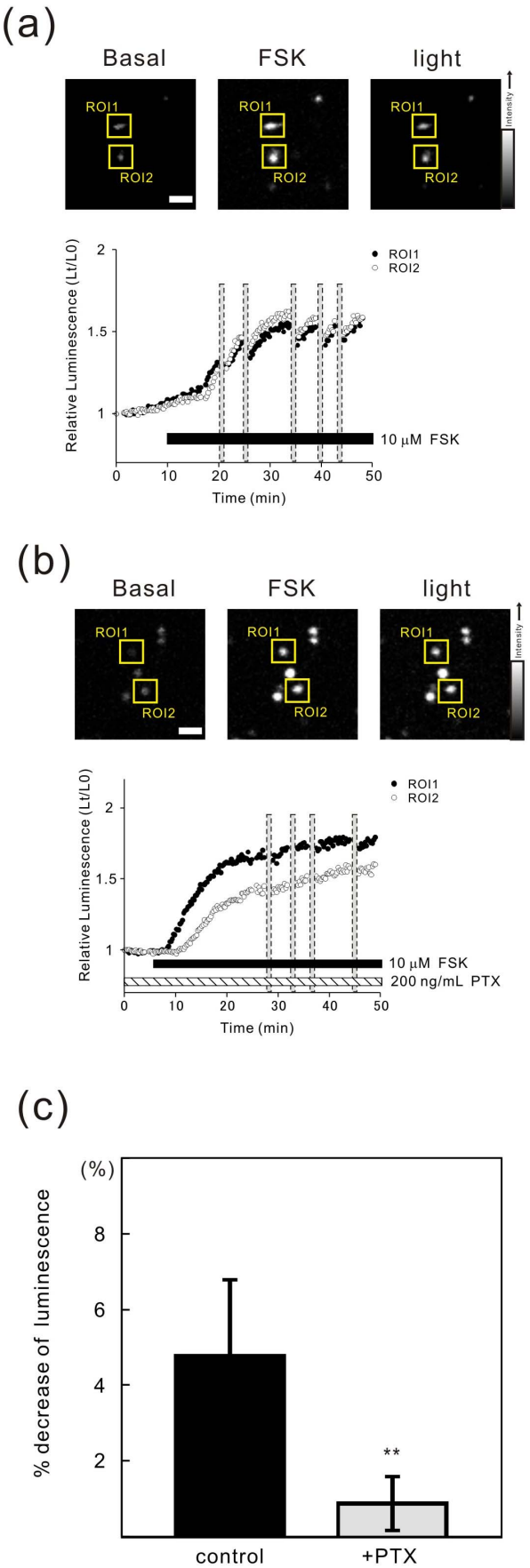

Figure 5 | Intracellular cAMP content decreases upon UV illumination in forskolin-stimulated cells. (a) OPN5-expressing HEK293 cells were transfected with cpGL-α-CT. Representative bioluminescence images acquired before (left) and after FSK treatment (centre), and after (right) UV light illumination are shown. The relative bioluminescence intensities (Lt/L0) from the cells in the indicated regions of interest (ROIs) were plotted. Treatment with 10 μM forskolin (FSK; black bar) increased the luminescence. Subsequent application of UV light (60 s at 0.2 μW/mm^2; shaded region) caused a transient decrease in luminescence. (b) The G_i-type G protein inhibitor, pertussis toxin (PTX; 200 ng/mL; hatched bar), blocked the UV light–induced decrease in luminescence. Representative imaging data are from 4 independent experiments. Bar = 50 μm. (c) Average decrease in bioluminescence of control and PTX-pre-treated cells. Average reduction from steady level of FSK-treated cells is shown. Light-induced luminescence change was significantly smaller in PTX-treated cells than in control cells (n = 20; $^{**}p < 0.01$).

expressing Neuro2a cells, we illuminated the cells with UV light after reconstitution with 11-*cis*-retinal. A 5-min exposure to UV light resulted in the phosphorylation of ERK1/2, p38 MAPK, and JNK/SAPK, and the phosphorylation progressively increased over 15 min of UV exposure in the OPN5-expressing cells (Fig. 6). This UV-induced MAPK phosphorylation was not seen in the empty vector controls or in the absence of 11-*cis*-retinal. These results demonstrated that the retinal-reconstituted OPN5 can serve as a UV-absorbing photoreceptor and induce the activation of MAPKs, such as ERK1/2, p38 MAPK, and JNK/SAPK.

Discussion

In this study, we developed a bioluminescence imaging technique using luciferase-based Ca^{2+} and cAMP indicators and demonstrated that UV illumination of human OPN5 induced a transient Ca^{2+} release from intracellular Ca^{2+} stores and a decrease in intracellular cAMP. The light-induced Ca^{2+} responses were confirmed by weak light fluorescent Ca^{2+} imaging using a conventional Ca^{2+} indicator Fluo-4. We also demonstrated that UV illumination induced the phosphorylation of MAPKs under dark conditions. These data suggest that UV light activation of OPN5 influences Ca^{2+} release, cAMP levels, and MAPK activation in cells.

Molecular imaging is a powerful tool for investigating intracellular signalling molecules, such as free Ca^{2+} and cAMP. Although fluorescent indicators of intracellular Ca^{2+} are widely used in imaging, as indicated by the present, light-induced cellular responses can be inadvertently affected by the wavelength(s) of light used to activate fluorescence during imaging. In this study, the bright blue light (470 nm) used to excite fuo-4 fluorescent indicator was probably sufficiently bright to directly activate the UV-absorbing OPN5 via the long-wavelength flank of its absorption spectrum. The basis for the maintained UV response using Calcium Orange is difficult to explain. Red light–shifted fluorescent indicators[17] have not been widely utilized, but they may help to address the issue of cross-activation in the future. In our study, we developed two new bioluminescent indicators based on firefly luciferase and demonstrated that they can be used to follow intracellular Ca^{2+} and cAMP dynamics in the drug-stimulated cells (Fig. 2). Although the temporal resolution of the bioluminescence imaging was limited because of weak luminescence activity of the indicators or the dynamic range of CCD apparatus, the time-lapse imaging of the changes in Ca^{2+} and cAMP levels could be performed in the present experimental condition. Moreover, we showed that weak light fluorescence imaging was suitable for investigating Ca^{2+} signalling though OPN5 activation. Employing these imaging techniques, we found that UV illumination induced an OPN5-mediated transient Ca^{2+} flux under dark conditions in OPN5-expressing HEK293 (Fig. 3a) and Neuro2a cells (Fig. 3e). Rat retinal cell line (RGC-5) endogenously expresses OPN5 gene and demonstrate a light-induced Ca^{2+} flux[6]. Differential light-induced Ca^{2+} responses were observed in RGC-5 cells: some population showed sustained Ca^{2+} elevation while a transient increase in Ca^{2+} was observed in other population. This difference in Ca^{2+} res-

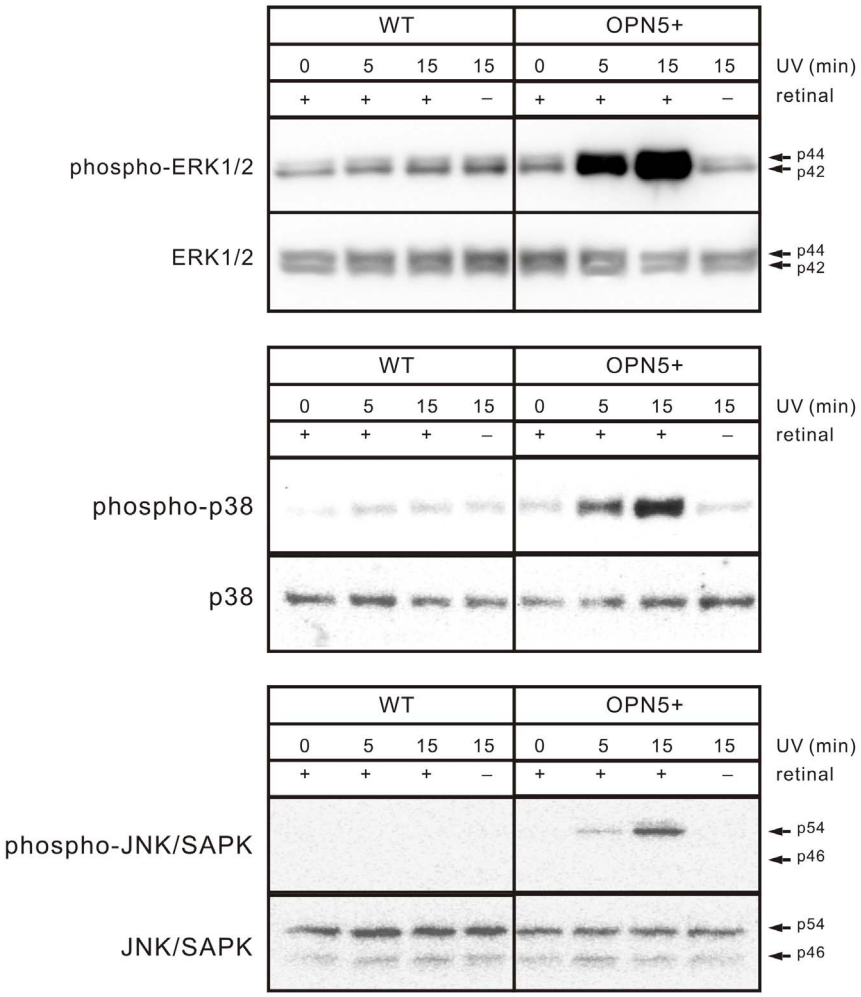

Figure 6 | Light-induced MAPK phosphorylation in OPN5-expressing Neuro2a cells. Empty vector–transfected (WT) and OPN5-expressing Neuro2a cells (OPN5+) were starved for 24 h in serum-free CO_2-independent medium in the dark with (+) or without (−) 11-*cis*-retinal (retinal) and harvested after the indicated times of exposure to UV light (λ_{max} = 352 nm; 1.23 μW/mm^2). Total cell lysates were subjected to western blotting with antibodies against phosphorylated or non-phosphorylated ERK1/2, p38, and JNK/SAPK. Western blots shown are representatives of 4 independent experiments for each antibody. The full length blots were presented in Supplementary Fig. S6.

ponse was thought to be caused by the differences in signalling molecules associated with OPN5 activation among the cell populations. In this study, we detected light-induced sustained Ca^{2+} flux by fluorescence imaging using Calcium Orange, and a transient increase of Ca^{2+} was detected by bioluminescence and weak light fluorescence imaging in OPN5-expressing HEK293 cells. The differences in Ca^{2+} response may be caused by the differences in signalling cascade associated with OPN5 activation. In addition, we found that OPN5 responded to repetitive light stimulation (Fig. 4a). Although another related human photoreceptor, OPN4/melanopsin, is also involved in light-induced transient Ca^{2+} increase, it does not respond to repetitive stimulation[18]. The differences in the response to repetitive light stimulation may have been caused by the differences in experimental conditions (bioluminescence imaging versus fluorescence imaging) rather than the differences in light-absorbance characteristics of opsin subtypes. We found that the Ca^{2+} source of OPN5-mediated Ca^{2+} flux is thapsigargin-sensitive intracellular Ca^{2+} stores (Fig. 4c). Although this is reminiscent of the coupling of OPN5 with a G_q-type G protein leading to intracellular Ca^{2+} flux observed in quail OPN5[2], a functional link between mammalian OPN5 and G_q-type G proteins has not yet been demonstrated.

It is also possible that human OPN5 signalling mechanism involves a $G_{i/o}$-type G protein. Many G protein–coupled receptors such as dopamine D2 receptor[18], noradrenaline α2 receptor[19], and serotonin 1A receptor[20] can activate both G_i and G_o proteins. These receptors not only inhibit adenylyl cyclase activity to reduce intercellular cAMP concentration but also activate the release of Ca^{2+} from Ca^{2+} stores. Our present study clearly demonstrated that photo-activation of OPN5 induces an increase in intracellular Ca^{2+} and reduction of cAMP (Figs. 3–5), but further experiments are required to uncover the precise molecular linkage underlying OPN5-mediated Ca^{2+} flux.

MAPKs belong to the serine/threonine protein kinase family that is activated by UV illumination. UV exposure induces the phosphorylation of ERK1/2, p38, and JNK/SAPK in keratinocytes[8] and JNK/SAPK phosphorylation in Neuro2a cells[21] at extremely high power. We found that UV exposure at relatively moderate power induced MAPK phosphorylation in OPN5-expressing cells but not in OPN5-negative cells. In other words, the sensitivity to UV light was increased by the expression of OPN5 gene.

It was recently reported that photo-induced increase in thyrotropin-stimulating hormone subunit β in birds is altered by RNA interference targeting OPN5[7]. The authors hypothesized that photo-induction may remove an inhibitory input from OPN5 and that this serves as an initial step in the functional link between light detection by a photoreceptive molecule and changes in the gene expression. As MAPKs are involved in the expression of the gene encoding corticotropin-releasing hormone in hypothalamic cells[22,23]

and corticotropin-releasing hormone plays an important role in inhibiting the secretion of thyrotropin-stimulating hormone[24], we speculate that OPN5 may regulate the secretion of reproductive hormones via the phosphorylation of MAPKs in birds.

Human and mouse OPN5 are UV-absorbing photopigments, and their potential role in the control of peripheral circadian rhythm have been investigated; however, UV exposure of OPN5-expressing outer ears of mice does not appear to affect biological rhythms[1]. Further investigation will help us to understand the physiological function of OPN5-mediated UV reception in mammals.

Methods

Reagents and vectors. Acetomethylated Fluo-4, Calcium Orange, and BAPTA were purchased from Invitrogen (Carlsbad, CA). Forskolin was obtained from Sigma-Aldrich (St. Louis, MO). D-Luciferin and pGL4.10 [*luc2*] vector were from Promega (Madison, WI). Thapsigargin, ATP, 11-*cis*-retinal, pertussis toxin, and other chemicals were from Wako Pure Chemical Industries, Ltd. (Osaka, Japan). Antibodies against ERK1/2, phospho-ERK1/2 (Thr202/Tyr204), p38 MAPK, phospho-p38 MAPK (Thr180/Tyr182), JNK/SAPK, phospho-JNK/SAPK (Thr183/Tyr185), and anti-rabbit secondary antibody conjugated with horseradish peroxidase were obtained from Cell Signaling Technology (Beverly, MA). Protein Assay kit was purchased from Bio-Rad Laboratories (Hercules, CA), and the ECL Prime Western Blotting Detection System was from GE Healthcare UK Ltd (Buckinghamshire, England).

Gene construction. Synthesized human OPN5 cDNA (1.2 kb) was purchased from Invitrogen and subcloned into the BamHI/EcoRI sites of vector pcDNA3.1(+) (Invitrogen) to make the mammalian expression vector.

To construct cpGL-α-CT, a fragment of mouse protein kinase A regulatory subunit Iα gene (amino acid residues L141–V381) was amplified by PCR, and the product was N-terminally fused to the C-terminal half (residues S399–V550) of the firefly luciferase (*luc2*; Promega), and was C-terminally fused to the N-terminal half (residues M1–G416) of *luc2*. A calmodulin-M13 fragment of cameleon, a genetically encoded Ca^{2+} indicator, was synthesized and inserted between the C- and N-terminal halves of luciferase to make cpGL-CaM. For bacterial and mammalian expression, these genes were subcloned into the BamHI/EcoRI sites of pRSET-B and pcDNA3.1(+) to construct pRSET-cpGL-CaM (-α-CT) and pcDNA-cpGL-CaM (-α-CT), respectively.

In Vitro titration of bioluminescent indicators. Recombinant proteins were purified from bacteria transformed with pRSET-cpGL-CaM or pRSET-cpGL-α-CT plasmids using QIAexpressionist (Qiagen), following the manufacturer's instructions. The concentration of purified protein was determined using Bio-Rad Protein Assay and diluted with a buffer consisting of 10 mM ethylene glycol-bis(2-aminoethylether)-N,N,N′,N′-tetraacetic acid (EGTA), 100 mM KCl, and 10 mM 3-morpholinopropane-1-sulfonic acid (MOPS; pH 7.2) to the concentration of 1 μg of protein/μL. Ca^{2+} titration was performed using Ca^{2+} calibration Buffer Kit (Invitrogen), according to manufacturer's manual. Briefly, 1 μg of recombinant protein was added to 50 μL of Ca^{2+} buffer and incubated for 10 min at room temperature (<24°C). Following incubation, 50 μL of sample was added to 50 μL of Luciferase Assay Reagent (Bright-Glo; Promega) solution and incubated further for 15 min at room temperature. Luminescence was measured using Luminescencer JNR (ATTO Corporation; Tokyo, Japan). For cAMP titration, 1 μg of purified protein was incubated with a dilution series of cNMP (cAMP or cGMP) in buffer consisting of 10 mM EGTA, 100 mM KCl, and 10 mM MOPS (pH 7.2) for 10 min at room temperature. Luciferase activity was measured by a method similar to that used for Ca^{2+} titration. The averaged data from 4 independent measurements were fitted using Microsoft Excel 2003 (Microsoft Corporation, Redmond, WA), and the results are expressed as mean ± SD.

Cell culture and transfection. Cell lines were obtained from ATCC (http://www.atcc.org/). HEK293 cells were grown in Modified Essential Medium with Earles salts (Invitrogen) supplemented with 10% fetal bovine serum, 1× non-essential amino acids, 50 U/mL penicillin, and 50 μg/mL streptomycin (all from Invitrogen). Neuruo2a cells were cultured in Dulbecco's Modified Eagle Medium (Invitrogen) supplemented with 10% fetal bovine serum, 50 U/mL penicillin, and 50 μg/mL streptomycin. For transient expression, cells were plated on a 35-mm glass-bottom dish (Iwaki; Chiba, Japan) and transfected with expression vectors (2 μg) using the FuGENE HD transfection reagent (Promega) and incubated at 37°C for 24–48 h in the medium.

To obtain HEK293 and Neuro2a cells stably expressing human OPN5, transfected cells were selected in the medium containing G418 (1 mg/mL; Invitrogen). G418-resistant cells were then grown in the medium, and OPN5 gene expression was analysed by reverse-transcription polymerase chain reaction (RT-PCR).

RT-PCR. Total RNA was isolated from ~10^9 OPN5-expressing cells and empty-vector-transfected cells using Trizol reagent (Invitrogen) followed by PureLink™ RNA Mini kit (Invitrogen), and 1 μg was used for each RT reaction using ReverTra Ace (Toyobo; Osaka, Japan). PCR was performed using 3 μL of the resulting cDNA in 10 μL of Ex Taq pre-mixed reaction solution (Takara Bio Inc.; Shiga, Japan). The PCR parameters were as follows: 94°C for 2 min; 30 cycles of 94°C for 30 s, 60°C for 30 s, and 72°C for 1 min; final extension at 72°C for 2 min. The PCR products were separated and analysed on a 2% agarose gel. The following primer sets were used for RT-PCR (OPN5) or PCR (GAPDH, positive control):

OPN5 Forward: 5′-GAAGCGGATTTAGTGGCTGGCTTTTACCTA-3′
OPN5 Reverse: 5′-CCAAGGGCATGGTGGTCCAGAAGGAAGCAT-3′
GAPDH Forward: 5′-ACCACAGTCCATGCCATCAC-3′
GAPDH Reverse: 5′-TCCACCACCCTGTTGCTGTA-3′.

Fluorescence Ca^{2+} imaging using a conventional fluorescence microscope. OPN5-expressing HEK293 cells were treated with 5 μM 11-*cis*-retinal in the medium for at least 60 min. Cells were rinsed twice with Basal Salt Solution (130 mM NaCl, 5.4 mM KCl, 2 mM $CaCl_2$, 1 mM $MgCl_2$, 10 mM D-glucose, and 10 mM HEPES, pH 7.4; Wako Pure Chemical Industries, Ltd.) and were loaded with Fluo-4 AM (5 μM) or Calcium Orange AM (5 μM). The cells were incubated for 60 min at room temperature (~24°C) in the dark room. Cells in the culture dishes were observed by an inverted microscope using a 40× objective lens (IX-81; Olympus; Tokyo, Japan). Fluo-4 and Calcium Orange were excited by light pulses through 470- to 490-nm and 520- to 550-nm band-pass filters, respectively.

The stimulating light from a 100-W halogen bulb was passed through 385- to 415-nm band-pass filter and low-pass filter (cut-off at 400-nm), and the light was guided to illuminate the microscope stage. Optical power on the stage was measured using an optical power meter (Advantest; Tokyo, Japan). For experiments involving light stimuli, fluorescence images were acquired immediately before and after (but not during) the light pulses to protect the camera from light overload.

Fluorescence images at 520 nm (Fluo-4) and 580 nm (Calcium Orange) were collected every 10 s using a charge-coupled device camera (ORCA2; Hamamatsu Photonics; Hamamatsu, Japan). Images were analysed using the MetaMorph software (Molecular Devices, LLC; Sunnyvale, CA). Each cell was chosen as a region of interest (ROI), and its fluorescence intensity at each time point was measured.

Weak light fluorescence and bioluminescence imaging. Cells were treated with 5-μM 11-*cis*-retinal in the medium for at least 60 min, and rinsed twice with Basal Salt Solution. Cells were loaded with Fluo-4 AM (5 μM) for fluorescence imaging or soaked in Basal Salt Solution supplemented with 2 mM D-luciferin for bioluminescence imaging in the dark room. The cells were allowed to stabilize for 60 min (Fluo-4) or 30 min (D-luciferin) prior to the experiment. The culture dish was placed on the stage of a microscopic luminescence imaging system (LuminoView LV200; Olympus), and cells were observed with a 40× objective and maintained at room temperature (~24°C) during the experiments. Fluo-4 was excited by light pulses (500 msec; 0.05 μW/mm²) through 470–490 nm band-pass filters from 100-W halogen bulb. The stimulation light was guided to the microscope stage, as described in Fluorescence Ca^{2+} imaging section.

Fluorescence and bioluminescence images were collected using a cooled electron-multiplying charge-coupled device camera (iXon; Andor Technology plc; Belfast, UK). Images were analysed using the MetaMorph software. Each cell was chosen as an ROI, and its fluorescence or luminescence intensity at each time point was measured.

UV exposure of cells and western blot analysis. The cells were seeded in 35-mm plastic culture dishes (1×10^5 cells/dish) and incubated in the medium for 24 h. After attachment of cells, the medium was changed to CO_2-independent medium (Invitrogen) supplemented with 2 μM 11-*cis*-retinal, and the cells were incubated at 37°C for 24 h in the dark. Cells were UV illuminated for 0, 5 or 15 min using UV lamp (λ_{max} = 352 nm; 1.23 μW/mm²; Toshiba lighting & Technology, Kanagawa, Japan). After irradiation, the cells were rinsed twice in ice-cold phosphate-buffered saline (pH 7.4) and incubated for 5 min in 0.5 mL ice-cold lysis buffer (150 mM NaCl, 0.1% SDS, 1% (v/v) Triton X-100, 50 mM Tris-HCl, pH 7.4) supplemented with Complete Protease Inhibitor Cocktail and PhosSTOP Phosphatase Inhibitor Cocktail (F. Hoffman-La Roche Ltd.; Basel, Switzerland). The cells were sonicated for 10 s on ice and centrifuged at 14,000 × *g* for 10 min at 4°C. The supernatant was collected and protein concentration determined using Bio-Rad Protein Assay.

For western blot analysis, 40 μg of each protein was subjected to SDS-PAGE (12.5% polyacrylamide) and transferred to a polyvinylidene difluoride membrane. The membrane was then blocked in blocking buffer (5% (w/v) non-fat dry milk, 0.1%(v/v) Tween-20, 150 mM NaCl, 20 mM Tris-HCl, pH 7.5) for 1 h at room temperature followed by overnight incubation at 4°C with appropriate primary antibody in blocking buffer (1 : 1000 dilution). The membrane was washed 3 times for 10 min each in a buffer containing 0.1% (v/v) Tween-20, 150 mM NaCl, and 20 mM Tris-HCl (pH 7.5), followed by incubation with horseradish peroxidase–conjugated anti-rabbit secondary antibody for 1 h. After three washes for 10 min each in a buffer containing 0.1% (v/v) Tween-20, 150 mM NaCl, and 20 mM Tris-HCl (pH 7.5), antibody-bound proteins on the membrane were detected by chemiluminescence detection (ECL Prime Western Blot Detection System) using Light Capture II (AE-6981FC; ATTO Corporation; Tokyo, Japan).

Statistical analysis. Statistical significance was determined using one-way ANOVA with Tukey's post hoc test.

1. Kojima, D. *et al.* UV-sensitive photoreceptor protein OPN5 in humans and mice. *PLoS One* **6**, e26388 (2011).

2. Nakane, Y. *et al.* A mammalian neural tissue opsin (Opsin 5) is a deep brain photoreceptor in birds. *Proc Natl Acad Sci U S A* **107**, 15264–15268 (2010).
3. Tarttelin, E. E., Bellingham, J., Hankins, M. W., Foster, R. G. & Lucas, R. J. Neuropsin (Opn5): a novel opsin identified in mammalian neural tissue. *FEBS Lett* **554**, 410–416 (2003).
4. Tsutsumi, M. *et al.* Expressions of rod and cone photoreceptor-like proteins in human epidermis. *Exp Dermatol* **18**, 567–570 (2009).
5. Yamashita, T. *et al.* Opn5 is a UV-sensitive bistable pigment that couples with Gi subtype of G protein. *Proc Natl Acad Sci U S A* **107**, 22084–22089 (2010).
6. Nieto, P. S., Valdez, D. J., Acosta-Rodriguez, V. A. & Guido, M. E. Expression of novel opsins and intrinsic light responses in the mammalian retinal ganglion cell line RGC-5. Presence of OPN5 in the rat retina. *PLoS One* **6**, e26417 (2011).
7. Stevenson, T. J. & Ball, G. F. Disruption of neuropsin mRNA expression via RNA interference facilitates the photoinduced increase in thyrotropin-stimulating subunit beta in birds. *Eur J Neurosci* **36**, 2859–2865 (2012).
8. Lopez-Camarillo, C. *et al.* Protein Kinases and Transcription Factors Activation in Response to UV-Radiation of Skin: Implications for Carcinogenesis. *Int J Mol Sci* **13**, 142–172 (2012).
9. Ong, W. K. *et al.* The activation of directional stem cell motility by green light-emitting diode irradiation. *Biomaterials* **34**, 1911–1920 (2013).
10. Cermakian, N. *et al.* Light induction of a vertebrate clock gene involves signaling through blue-light receptors and MAP kinases. *Curr Biol* **12**, 844–848 (2002).
11. Welsh, D. K. & Noguchi, T. Cellular bioluminescence imaging. *Cold Spring Harb Protoc* **2012**, (2012).
12. Kaihara, A., Umezawa, Y. & Furukawa, T. Bioluminescent indicators for Ca^{2+} based on split Renilla luciferase complementation in living cells. *Anal Sci* **24**, 1405–1408 (2008).
13. Binkowski, B., Fan, F. & Wood, K. Engineered luciferases for molecular sensing in living cells. *Curr Opin Biotechnol* **20**, 14–18 (2009).
14. Binkowski, B. F. *et al.* A luminescent biosensor with increased dynamic range for intracellular cAMP. *ACS Chem Biol* **6**, 1193–1197 (2011).
15. Binkowski, B. F., Fan, F. & Wood, K. V. Luminescent biosensors for real-time monitoring of intracellular cAMP. *Methods Mol Biol* **756**, 263–271 (2011).
16. Fan, F. *et al.* Novel genetically encoded biosensors using firefly luciferase. *ACS Chem Biol* **3**, 346–351 (2008).
17. Egawa, T. *et al.* Development of a far-red to near-infrared fluorescence probe for calcium ion and its application to multicolor neuronal imaging. *J Am Chem Soc* **133**, 14157–14159 (2011).
18. Hartwick, A. T. *et al.* Light-evoked calcium responses of isolated melanopsin-expressing retinal ganglion cells. *J Neurosci* **27**, 13468–13480 (2007).
19. Strosberg, A. D. Structure, function, and regulation of adrenergic receptors. *Protein Sci* **2**, 1198–1209 (1993).
20. Gerhardt, C. C. & van Heerikhuizen, H. Functional characteristics of heterologously expressed 5-HT receptors. *Eur J Pharmacol* **334**, 1–23 (1997).
21. Mielke, K., Damm, A., Yang, D. D. & Herdegen, T. Selective expression of JNK isoforms and stress-specific JNK activity in different neural cell lines. *Brain Res Mol Brain Res* **75**, 128–137 (2000).
22. Blume, A. *et al.* Prolactin activates mitogen-activated protein kinase signaling and corticotropin releasing hormone transcription in rat hypothalamic neurons. *Endocrinology* **150**, 1841–1849 (2009).
23. Singru, P. S., Sanchez, E., Acharya, R., Fekete, C. & Lechan, R. M. Mitogen-activated protein kinase contributes to lipopolysaccharide-induced activation of corticotropin-releasing hormone synthesizing neurons in the hypothalamic paraventricular nucleus. *Endocrinology* **149**, 2283–2292 (2008).
24. Tsigos, C. & Chrousos, G. P. Hypothalamic-pituitary-adrenal axis, neuroendocrine factors and stress. *J Psychosom Res* **53**, 865–871 (2002).

Acknowledgments

We thank Dr. T. Kinebuchi and Ms. Y. Ohashi for their suggestions regarding the bioluminescence imaging and Dr. S. Karaki for her management and encouragement. We also thank Life Technologies Corporation (http://www.lifetechnologies.com/) for permission to use the spectral data of fluorescent Ca^{2+} indicators.

Author contributions

T.S., H.S. and T.T. designed and performed the experiments. T.S. analysed the data and wrote the manuscript.

Additional information

Supplementary information accompanies this paper at http://www.nature.com/scientificreports

Competing financial interests: The authors are employees of Olympus Corporation, and this work was funded by Olympus Corporation.

How to cite this article: Sugiyama, T., Suzuki, H. & Takahashi, T. Light-induced rapid Ca^{2+} response and MAPK phosphorylation in the cells heterologously expressing human OPN5. *Sci. Rep.* **4**, 5352; DOI:10.1038/srep05352 (2014).